# Correlation between Photoreceptor Layer Integrity and Visual Function in Patients with Stargardt Disease: Implications for Gene Therapy

*Francesco Testa,*[1,2] *Settimio Rossi,*[1,2] *Andrea Sodi,*[3] *Ilaria Passerini,*[4] *Valentina Di Iorio,*[1] *Michele Della Corte,*[1] *Sandro Banfi,*[5,6] *Enrico Maria Surace,*[5] *Ugo Menchini,*[3] *Alberto Auricchio,*[5,7] *and Francesca Simonelli*[1,5]

**Purpose.** To perform a clinical characterization of Stargardt patients with *ABCA4* gene mutation, and to investigate the correlation between the inner and outer segment (IS/OS) junction morphology and visual acuity, fundus lesions, electroretinogram abnormalities, and macular sensitivity.

**Methods.** Sixty-one patients with Stargardt disease (STGD) were given a comprehensive ophthalmic examination. Inner-outer photoreceptor junction morphology evaluated by spectral-domain optical coherence tomography was correlated with visual acuity, fundus lesions, fundus autofluorescence, full-field and multifocal electroretinography responses, and microperimetric macular sensitivities. We classified STGD patients into three groups: (1) IS/OS junction disorganization in the fovea, (2) IS/OS junction loss in the fovea, and (3) extensive loss of IS/OS junction. Mutation analysis of the *ABCA4* gene was carried out by sequencing the complete coding region.

**Results.** A significant difference in visual acuity was observed between IS/OS groups 1 and 2 and between IS/OS groups 2 and 3 ($P < 0.0001$). A significant difference in microperimetry sensitivity was observed between IS/OS groups 2 and 3, and between IS/OS groups 1 and 3 ($P < 0.0001$). There was also a statistically significant correlation between IS/OS abnormalities and the extent of fundus lesions (Spearman $P \leq 0.01$), as well as with the type of ERG and multifocal ERG results (Spearman $P \leq 0.01$). Finally, the degree of IS/OS junction preservation showed a statistically significant correlation with the extension of foveal abnormalities assessed by fundus autofluorescence imaging (Spearman $P \leq 0.01$). The G1961E mutation was more frequent in the patients without extensive loss of IS/OS junction ($P = 0.01$) confirming its association with a milder STGD phenotype.

**Conclusions.** The results of this study suggest that a comprehensive approach in the examination of Stargardt patients has the potential to improve the understanding of vision loss and may provide a sensitive measure to evaluate the efficacy of future experimental therapies in patients with STGD. (*Invest Ophthalmol Vis Sci.* 2012;53:4409–4415) DOI:10.1167/iovs.11-8201

Stargardt disease (STGD) is an autosomal-recessive macular disease characterized by excessive accumulation of lipofuscin in the RPE.[1,2] The general course of STGD is a slow loss of central vision due to central atrophy and thus loss of central visual function.[3–5] It has been recognized that STGD is associated with mutations in the *ABCA4* gene, which encodes a transport protein located in the rim of photoreceptor discs and is involved in the transport of all-trans retinal through the disc membrane. ABCA4 protein dysfunction determines accumulation of all-trans retinal in the photoreceptors and in the RPE, following the phagocytosis of the photoreceptor outer segments by RPE. All-trans retinal is converted to A2-E, a major component of lipofuscin, which determines a toxic effect on RPE and overlying photoreceptors.[6,7] Even if both RPE and photoreceptor layers are involved in the pathogenesis of STGD, from a clinical viewpoint the assessment of photoreceptor function is one of the most important aspects of the disease.

Therefore, a method that correlates the fundus status with functional variables could be useful for a more accurate evaluation of disease severity. To date, clinical diagnosis is mainly based on biomicroscopy, fluorescein angiography, fundus autofluorescence imaging, and multifocal electroretinography. However, none of these methods alone can actually show the amount of photoreceptor loss, which would be essential for future therapeutic applications particularly in the case of gene therapy. The recent introduction of spectral domain optical coherence tomography (SD-OCT) allows the examination of retinal layers with micrometer resolution and the precise visualization of retinal features, which can be correlated with functional data and with disease-associated genotypes.[8]

The purpose of this study was to perform an extensive clinical characterization of Stargardt patients with *ABCA4* gene mutation, and to investigate the correlation between the inner-outer photoreceptor junction morphology, as determined by SD-OCT, and other clinical parameters, such as visual acuity,

From the [1]Department of Ophthalmology, and [6]Medical Genetics, Department of General Pathology, Seconda Università degli Studi di Napoli, Naples, Italy; [3]Department of Oto-Neuro-Ophthalmological Surgical Sciences, University of Florence, Florence, Italy; [4]Department of Genetic Diagnostics, Careggi University Hospital, Florence, Italy; [5]Telethon Institute of Genetics and Medicine (TIGEM), Naples, Italy; and [7]Medical Genetics, Department of Pediatrics, Federico II University, Naples, Italy.

[2]These authors contributed equally to this work and should therefore be regarded as equivalent authors.

Supported by National Institutes of Health Grant 1 R24 EY019861-01A1.

Submitted for publication July 11, 2011; revised December 1, 2011, March 13 and May 18, 2012; accepted May 20, 2012.

Disclosure: **F. Testa**, None; **S. Rossi**, None; **A. Sodi**, None; **I. Passerini**, None; **V. Di Iorio**, None; **M. Della Corte**, None; **S. Banfi**, None; **E.M. Surace**, None; **U. Menchini**, None; **A. Auricchio**, None; **F. Simonelli**, None

Corresponding author: Francesca Simonelli, Department of Ophthalmology, Seconda Università degli Studi di Napoli, Via S Pansini 5, 80131 - Naples, Italy; franctes@tin.it.

fundus lesions found by biomicroscopy, fundus autofluorescence, electroretinogram abnormalities, and macular sensitivity assessed by microperimetry. By means of SD-OCT data, two categories of patients were recognized, defining two stages of disease; thus, the different prevalence of *ABCA4* gene mutations in these two groups of STGD patients was also evaluated.

## Methods

### Patient Selection and Phenotype Analysis

Sixty-one patients diagnosed with STGD from 50 families were ascertained through the Referral Center for Hereditary Retinopathies of the Department of Ophthalmology of the Second University of Naples, Italy. The study adhered to the tenets of the Declaration of Helsinki and was approved by the Local Ethics Committees. Moreover, each patient gave written informed consent for his or her involvement.

The clinical examination included the following tests: best corrected visual acuity (BCVA) with manifested refraction by Snellen visual chart, slit-lamp biomicroscopy of anterior segment and fundus examination, full-field ERG, multifocal ERG (mfERG), microperimetry, SD-OCT, and fundus autofluorescence (FAF).

The clinical diagnosis of STGD was based on a recorded family history compatible with autosomal recessive inheritance, presence of bilateral impairment of central vision, atrophic macular lesions (a beaten bronze appearance or large patches of atrophy) with or without the appearance of perimacular and/or peripheral white-yellow flecks and normal to subnormal ERG.

Fundus lesions ascertained by biomicroscopy were classified according to Fishman et al.[9] as follows: (1) phenotype I included patients with a small atrophic-appearing foveal lesions and localized perifoveal yellowish-white flecks; (2) phenotype II included patients with numerous yellowish-white fundus lesions throughout the posterior pole; and (3) phenotype III included patients with extensive atrophic-appearing RPE changes.

Full-field ERG was recorded by corneal contact lens electrodes with a Ganzfeld stimulator (EREV 2000 Electrophysiology system; LACE Elettronica, Pisa, Italy) according to the recommendation of the International Society for Clinical Electrophysiology of Vision (ISCEV).[10] ERG abnormalities were classified into three groups based on the following criteria proposed by Lois et al.[11]: group 1 had normal full-field amplitudes; group 2 had normal scotopic rod ERG but reduced photopic b-wave amplitudes; and group 3 had ERG abnormalities involving both rods and cones.

Multifocal ERG was performed by Veris Science 6.1 system (EDI, Inc., San Mateo, CA) according to ISCEV standards using DTL electrodes and a stimulus array of 103 hexagons.[12] On the basis of the response densities at different retinal eccentricities and considering the results obtained in photopic Ganzfeld ERG, the following functional staging was applied according to Kretschmann et al.[13]: class I, subnormal mfERG only in eccentric groups 1 and 2 (0°–7°); class II, subnormal mfERG in eccentric groups 1, 2, and 3 (0°–12°); class III, subnormal mfERG in the entire test field (0°–30°), but normal Ganzfeld ERG; and class IV, subnormal mfERG in the entire test field (0°–30°) plus pathologic Ganzfeld ERG.

SD-OCT (Cirrus HD-OCT; Carl Zeiss, Dublin, CA) was performed on 61 patients. The acquisition protocol comprised both a five-line raster scan and a macular cube scan pattern (512 × 128 pixels) in which a 6 × 6-mm region of the retina was scanned within a scan time of 2.4 seconds. Patients with a signal strength ≤8 were excluded ($n = 10$). The retinal thickness analysis protocol provided with the instrument software was used to calculate the foveal thickness. Based on the morphology of the inner-outer segment (IS/OS) junction layer of the photoreceptors (a band of high-reflectance, inner to the RPE layer),[14] we classified STGD patients into three categories: (1) IS/OS junction disorganization in the fovea, (2) IS/OS junction loss in the foveal area, and (3) extensive loss of IS/OS junction (more than 1 disc diameter from the fovea). The IS/OS in the SD-OCT images was evaluated in each patient on the same horizontal scan through the center of the fovea.

Microperimetry was performed on all subjects using an automatic fundus-related perimeter (MP1 Microperimeter; Nidek Technologies, Padova, Italy). For the purpose of this study, the following parameters were used: a fixation target of 2° in diameter consisting of a red ring; a white, monochromatic background with a luminance of 4 abs; and a Goldman III–size stimulus with a projection time of 200 ms. The stimulus was randomly projected according to a customized radial grid of 61 points covering the central portion of the retina (10° centered onto the fovea; points aligned on the 0°, 30°, 60°, 90°, 120°, and 150° radial axes, 1° apart), and a 4-2-1 double staircase strategy was used with an automatic eye tracker that compensated for eye movements.[15]

Autofluorescence images of 47 patients were also obtained, using a confocal scanning laser ophthalmoscope (Heidelberg Retina Angiograph; Heidelberg Engineering, Heidelberg, Germany). Thirty-degree field-of-view images were recorded after pupillary dilation. Standard procedure was followed for the acquisition of FAF images, including focus of the retinal image. An argon laser light (488 nm) was used for illumination, and a wide-band pass filter with cut-off at 500 nm was present in front of the detector. A series of nine FAF images 30° × 30° encompassing the entire macular area with at least a portion of the optic disc, were recorded, digitalized, aligned for eye movements, and averaged to produce a single frame with improved signal-to-noise ratio. Based on FAF findings, the macular lesions were further divided into three groups based on the following criteria: (1) the presence of a ring of increased autofluorescence surrounding an area of decreased autofluorescence; (2) the absence of foveal autofluorescence (<1 disc diameter); and (3) the absence of macular autofluorescence (≥2 disc diameter).

### Mutation Analysis

A complete family history was recorded for the genetic analysis, and 10 mL peripheral blood was obtained from the antecubital vein using EDTA-containing vials. DNA was extracted from 200 μL peripheral blood with Biorobot EZ1 (QIAGEN GmbH, Hilden, Germany).

Coding regions, intron/exon boundaries, and 5′ and 3′ regions of *ABCA4* were amplified in 50 reactions. The PCR amplification was performed using the Core System-Robotic Station (Beckman Coulter, Miami, FL). Cycling parameters for each reaction were optimized for all the exons. The PCR amplification of 50 exons and flanking intronic regions of the *ABCA4* gene was performed using 50 to 100 ng of genomic DNA. Amplification was performed in 50 mM KCl, 10 mM Tris-HCl, pH 8.3, 5 mM $MgCl_2$, 200 M dNTPs, and 0.5 M for each primer set. AmpliTaq DNA polymerase (1 U AmpliTaq Gold; Applied Biosystems, Foster City, CA) was added for each 25-L reaction. PCR was performed by a multi-block MWG PCR System (Eurofins MWG Operon, Ebersberg, Germany); cycling parameters for the reactions were optimized for each exon. PCR products were purified by Biomek NX station (Beckman Coulter).

Standard cycle-sequencing reactions with BigDye Terminator Mix (v1.1; Applied Biosystems, Foster City, CA) contained 3 to 10 ng purified PCR products in 20 μL dye-terminator reaction mixture and were performed with forward and reverse primers used for initial amplification. The sequencing reactions were precipitated by Biomek NX station, then dried and sequenced on a sequencer 3730 DNA Analyzer (Applied Biosystems). Finally, data obtained from the Sequence Analysis Software (Applied Biosystems) were aligned with the wild-type *ABCA4* gene sequence (GenBank Database, in the public domain; http://www.ebi.ac.uk/queries/bq.html). According to EMQN Best Practice Guidelines, a sequence mismatch was considered as a disease-causing mutation only if absent in 300 healthy controls, associated with amino acidic change, and confirmed by a new independent PCR. Segregation analysis was performed in all families to determine the phase for all mutations.

**Table 1.** Clinical and Molecular Data of STGD Patients

| Patient ID/Fam | Age (y) | Visual Acuity | OCT ft (μm) | MP (dB) | IS/OS* | Fundus† | FAF‡ | ERG§ | mfERG‖ | Mutation 1 | Mutation 2 |
|---|---|---|---|---|---|---|---|---|---|---|---|
| 4/2 | 50 | 0.0715 | 134 | 5.25 | – | 1 | – | 2 | 4 | G1961E | 250InsCAAA |
| 5/2 | 47 | 0.1 | 127 | 14.2 | 2 | 1 | 1 | 1 | 3 | G1961E | 250InsCAAA |
| 6/3 | 33 | 0.05 | 125 | 9.8 | 2 | 2 | 2 | 1 | 3 | G1961E | R2149X |
| 7/4 | 18 | 0.085 | 135 | 0 | – | 2 | – | 3 | 4 | 5917del G | 5917del G |
| 8/5 | 16 | 0.095 | 104 | 0.9 | 3 | 2 | 3 | 3 | 4 | L541P; A1038V | L541P; A1038V |
| 9/6 | 71 | 0.03 | 109 | 0 | 3 | 3 | 3 | 2 | 4 | IVS35+2t > c | G1961E |
| 11/7 | 46 | 0.2 | 137 | 9.35 | 2 | 1 | 2 | 1 | 1 | Y850K | A1598D |
| 13/8 | 35 | 0.017 | 163 | 0 | – | 3 | – | 3 | 4 | L541P | R1098C |
| 15/10 | 20 | 0.1 | 135.5 | 11.05 | 2 | 1 | 1 | 1 | 4 | IVS35+2t > c | G1961E |
| 16/11 | 20 | 0.47 | 96 | 16.7 | 2 | 1 | 2 | 1 | 2 | L541P; A1038V | L541P; A1038V |
| 17/11 | 34 | 0.1 | 114.5 | 7.55 | 2 | 1 | 2 | 1 | 3 | L541P; A1038V | L541P; A1038V |
| 18/11 | 18 | 1 | 134 | 16.15 | 1 | 1 | 1 | 1 | 3 | L541P; A1038V | L541P; A1038V |
| 19/12 | 12 | 0.12 | 242 | 6.5 | 3 | 1 | 2 | 1 | 2 | L541P; A1038V | L541P; A1038V |
| 20/13 | 28 | 0.1 | 111 | 14.2 | 2 | 2 | 2 | 1 | 3 | R1443H | IVS35+2t > c |
| 21/14 | 34 | 0.2 | 152 | 14.15 | 2 | 1 | 2 | 2 | 4 | R653C | G1961E |
| 22/15 | 69 | 0.079 | 122 | 0 | 3 | 3 | 3 | 3 | 4 | I1562T | R2149X |
| 23/15 | 46 | 0.55 | 162 | 1.05 | 3 | 3 | 3 | 3 | 4 | I1562T | IVS45+1g > c |
| 25/16 | 28 | 0.11 | 105.5 | 3.1 | 3 | 2 | 2 | 3 | 4 | R212C | R212C |
| 26/17 | 13 | 0.084 | 138.5 | 0.2 | 3 | 2 | 3 | 1 | 3 | R18W | C1490Y |
| 27/4 | 20 | 0.0775 | 131 | 0 | – | 3 | – | 3 | 4 | 5917del G | 5917del G |
| 28/4 | 23 | 0.042 | 159.5 | 0 | – | 3 | – | 3 | 4 | 5917del G | 5917del G |
| 30/18 | 29 | 0.0375 | 103 | 0 | 3 | 3 | 3 | 3 | 4 | N965S | G1961E |
| 31/19 | 17 | 0.1 | 102 | 9 | 3 | 2 | 2 | 3 | 4 | L541P | F655C |
| 38/20 | 20 | 0.225 | 95 | 16 | 2 | 1 | 1 | 3 | 4 | L541P | G1961E |
| 39/21 | 20 | 0.17 | 146 | 16.7 | 2 | 1 | 1 | 1 | 3 | G1961E | R2030X |
| 42/22 | 43 | 0.575 | 127 | 7.05 | 2 | 1 | 2 | 1 | 2 | 250insCAAA | G1961E |
| 43/23 | 12 | 0.1 | 117.5 | 11.55 | 2 | 2 | 2 | 1 | 3 | IVS40+5g > a | IVS15-8g > a |
| 44/24 | 29 | 0.1 | 149 | 18.5 | 2 | 1 | 2 | 1 | 3 | G1961E | 4736del6bpins2bp |
| 46/25 | 38 | 0.0075 | 182.5 | 0 | – | 3 | – | 3 | 4 | G618R | G1972R |
| 48/26 | 35 | 0.46 | 133.5 | 12.25 | 2 | 1 | – | 1 | 3 | 4538insC | G1961E |
| 50/27 | 13 | 0.2 | 122.5 | 17.35 | 2 | 1 | 2 | 1 | 3 | IVS35+2t > c | G1961E |
| 51/28 | 24 | 0.065 | 123 | 0 | 3 | 3 | 3 | 3 | 4 | 250InsCAAA | V767D |
| 52/29 | 14 | 1 | 147 | 6.15 | 1 | 1 | 1 | 3 | 4 | L2027F | A1881V |
| 53/30 | 45 | 0.1 | 120 | 6.05 | 3 | 2 | 2 | 1 | 3 | G1961E | R2030X |
| 54/30 | 24 | 0.09 | 159 | 2.65 | 3 | 3 | 3 | 3 | 4 | V767D | R2030X |
| 55/31 | 34 | 0.085 | 150 | 5.15 | 3 | 3 | 3 | 3 | 4 | N96H | IVS40+5g > a |
| 56/32 | 48 | 0.0335 | 118.5 | 4.4 | – | 3 | – | 2 | 4 | IVS35+2t > c | G1961E |
| 58/32 | 52 | 0.05 | 124 | 5.8 | 3 | 2 | 2 | 2 | 4 | IVS35+2t > c | G1961E |
| 60/33 | 43 | 0.065 | 163 | 15.95 | 2 | 1 | – | 1 | 2 | 250InsCAAA | G1961E |
| 61/34 | 45 | 0.03 | 187.5 | 4.5 | 1 | 1 | 1 | 2 | 1 | R1640Q | G1961E |
| 64/35 | 33 | 0.0665 | 158 | 0 | 3 | 3 | 3 | 3 | 4 | C2150R | 2626InsTTT |
| 65/35 | 38 | 0.008 | 172 | 0.05 | 3 | 3 | 3 | 3 | 4 | C2150R | 2626InsTTT |
| 66/36 | 42 | 0.4 | 137 | 0.95 | 3 | 2 | 2 | 1 | 3 | N96D | IVS40+5g > a |
| 67/37 | 14 | 0.235 | 132 | 0.15 | 3 | 2 | 3 | 3 | 4 | IVS6-2a > t | IVS6-2a > t |
| 69/38 | 19 | 0.09 | 120 | 0 | 3 | 1 | 2 | 1 | 3 | R511H | N529S |
| 70/39 | 42 | 0.515 | 140 | 0.4 | 3 | 3 | 3 | 3 | 4 | IVS40+5g > a | N965S |
| 72/40 | 33 | 0.096 | 116.5 | 5.1 | 3 | 2 | 2 | 1 | 3 | N96D | L2140Q |
| 73/41 | 17 | 0.1 | 160 | 14.35 | 2 | 2 | 2 | 3 | 4 | G690D | A1598D |
| 74/42 | 36 | 0.0125 | 142.5 | 0 | 3 | 3 | 3 | 3 | 4 | N96H | N96H |
| 75/43 | 45 | 0.2 | 214.5 | 11.7 | 2 | 1 | 2 | 1 | 3 | IVS35+2t > c | G1961E |
| 77/44 | 19 | 0.34 | 137.5 | 11.75 | 2 | 1 | – | 1 | 3 | G1961E | G618R |
| 81/45 | 66 | 0.335 | 163 | 2 | – | 3 | – | 2 | 4 | N96D | G1961E |
| 82/46 | 41 | 0.1 | 116.5 | 0.15 | 3 | 3 | 3 | 3 | 4 | 4538insC | IVS40+5g > a |
| 83/47 | 17 | 0.395 | 165 | 19.25 | 1 | 1 | 1 | 1 | 2 | G1961E | IVS45+1g > c |
| 84/47 | 26 | 0.135 | 120 | 16.2 | 2 | 1 | 2 | 1 | 3 | G1961E | IVS45+1g > c |
| 85/48 | 10 | 0.16 | 149.5 | 12.4 | 2 | 2 | 2 | 1 | 3 | IVS35+2t > c | IVS40+5g > a |
| 87/40 | 25 | 0.9 | 155 | 15 | 2 | 1 | 2 | 1 | 2 | N96D | L2140Q |
| 88/49 | 32 | 0.0715 | 144 | 0.1 | – | 3 | – | 3 | 4 | IVS45+1g > c | R2149X |
| 89/50 | 14 | 0.1185 | 147 | 1.85 | 3 | 1 | – | 3 | 4 | P402A | 250insCAAA |
| 90/51 | 35 | 0.07 | 116.5 | 0 | – | 3 | – | 3 | 4 | A1598D | R2030X |
| 94/52 | 30 | 0.1 | 144 | 12.85 | 2 | 1 | – | 1 | 1 | A1598D | G1961E |

Fam, family; OCT ft, optical coherence tomography foveal thickness; MP, microperimetry; IS/OS, inner–outer segment junction; FAF, fundus autofluorescence; ERG, electroretinogram; mfERG, multifocal-electroretinogram.

* IS/OS: (1) IS/OS junction disorganization in the fovea, (2) IS/OS junction loss in the foveal area, and (3) extensive loss of IS/OS junction (more than 1 disc diameter from the fovea).

† Fundus: (1) small atrophic-appearing foveal lesion and localized perifoveal yellowish-white flecks; (2) numerous yellowish-white fundus lesions throughout the posterior pole; (3) extensive atrophic-appearing RPE changes.

‡ FAF: (1) presence of a ring of increased autofluorescence surrounding an area of decreased autofluorescence; (2) absence of foveal autofluorescence (<1 disc diameter); and (3) absence of macular autofluorescence (≥2 disc diameter).

§ ERG: (1) normal full field amplitudes; (2) normal scotopic but reduced photopic b wave amplitudes; (3) abnormal responses involving both rods and cones.

|| mfERG: (1) subnormal mfERG only in eccentric groups 1 and 2 (0°–7°); (2) subnormal mfERG in eccentric groups 1, 2, and 3 (0°–12°); (3) subnormal mfERG in the entire test field (0°–30°), but normal Ganzfeld ERG; (4) subnormal mfERG in the entire test field (0°–30°) plus pathologic Ganzfeld ERG.

## Statistics

Our set of data is described by continuous (BCVA, OCT foveal thickness, and macular sensitivities) and categorical (fundus, FAF, IS/OS, ERG, and mfERG groups) variables. Since there were no significant differences (BF > 1; Bayesian *t*-test), between right- and left-eye values of visual acuity, OCT foveal thickness, and macular sensitivity, we used average values between right and left eyes. Furthermore, there were no differences between the two eyes as regards ERG classification (according to Lois et al.)[11] and mfERG (according to Kretschmann et al.).[13]

The difference between the means of the continuous variables was tested via one-way ANOVA with IS/OS group as factor and post hoc Tukey test, when appropriate. Continuous variable normality was assessed by Shapiro–Wilk normality test ($P < 0.001$). For categorical variables, the Freeman–Halton extension of the Fisher exact probability test was adopted.

Spearman rank correlation test was used to evaluate the following correlations:

- OCT foveal thickness versus IS/OS groups, BCVA, fundus groups, ERG groups, mfERG groups, FAF groups, and retinal mean sensitivity;
- age of patients versus IS/OS groups, BCVA, fundus groups, ERG groups, mfERG groups, FAF groups, and retinal mean sensitivity;
- IS/OS junction alteration versus BCVA, fundus groups, ERG groups, mfERG groups, FAF groups, and retinal mean sensitivity.

Student's *t*-test was used to evaluate the difference in age among the STGD groups classified according to the IS/OS junction abnormalities. IS/OS abnormalities compared with patient age was performed combining groups 1 and 2 (Group I) versus group 3 (Group II) in order to obtain two numerically comparable groups.

Three different Fisher exact tests were used to evaluate the significance of association (contingency) between the Group I/II classification and the presence/absence of missense mutation, premature truncation, and/or G1961E.

## Results

Table 1 summarizes all clinical data and the detected *ABCA4* disease-associated alleles of STGD patients. Eighty-nine of these alleles represented missense mutations, whereas the remaining 42 were predicted to lead to a premature truncation of the ABCA4 protein. Molecular analysis revealed six new, previously not described, mutations in the *ABCA4* gene (Y850K; A1881V; N529S; R511H; IVS15-8g > a; IVS6-2a > t).

The median BCVA, evaluated in all patients, was Snellen 0.05 (20/400), range 0.01 to 1 (20/1920 to 20/20), for the right eye and 0.06 (20/340), range 0.008 to 1 (20/2400 to 20/20), for the left eye.

Ophthalmoscopic lesions were consistent with Fishman 1 in 26 STGD patients (42.6%), with Fishman 2 in 15 patients (24.6%), and with Fishman 3 in 20 patients (32.8%). The ERG tracing showed different degrees of abnormalities among patients: 28 patients (45.9%) showed a type-1 ERG response; 7 patients (11.5%), a type-2 ERG; and the remaining 26 (42.6%), a type-3 ERG. Also, mfERG showed different classes of abnormalities among patients: 3 patients (4.9%) showed a class-1 mfERG response; 6 patients (9.8%), a class-2; 19 patients (31.2%), a class-3; and the remaining 33 (54.1%), a class-4 response.

OCT examination revealed that the mean central foveal thickness was reduced in all patients (141 ± 27 μm; normal value 271.4 ± 19.6 μm).

Evaluation of IS/OS junction was obtained only in 51 patients because the OCT signal strength recorded in the remaining 10 patients was ≤8; IS/OS junction disorganization in the fovea was found in 4 patients (7.8%; Fig. 1a); IS/OS junction loss was found in the foveal area in 23 patients (45.1%; Fig. 1b); and extensive loss of IS/OS junction was found in the remaining 24 (47.1%; Fig. 1c).

FAF imaging was obtained only in 46 patients, because 15 patients were not willing to undergo FAF testing. The presence of a ring of increased autofluorescence surrounding an area of decreased autofluorescence (group 1) was observed in 8 patients (17.4%; Fig. 1d); absence of foveal autofluorescence (group 2) in 23 patients (50%; Fig. 1e); and absence of macular autofluorescence (group 3) in 15 patients (32.6%; Fig. 1f).

Mean macular sensitivities determined by microperimetry revealed a decreased visual sensitivity in all patients (6.3 dB ± 6.4 SD) ranging from 0 to 19.2 dB (normal value 19.6 ± 0.4 dB).

ANOVA revealed a significant difference in visual acuity ($P \leq 0.0001$) and retinal sensitivity ($P \leq 0.0001$) between the three IS/OS groups. The post hoc Tukey test showed that this result was due to the difference between groups 1 and 2, and groups 1 and 3 for visual acuity (Fig. 2a); and between groups 2 and 3, and groups 1 and 3 for retinal sensitivity (Fig. 2b). On the contrary, the analysis on macular thickness, considering IS/OS as factors, showed that there is no significant difference between the three IS/OS groups ($P = 0.31$).

The Freeman-Halton extension of the Fisher exact probability test showed the association between the IS/OS factor and each of the other categorical clinical parameters selected in the study (i.e., FAF, Fundus, ERG, and mfERG groups). Each test showed a $P$ value < 0.0001.

Moreover, we correlated the different retinal abnormalities detected by OCT both in terms of macular thickness and preservation of IS/OS junction with BCVA, microperimetry macular sensitivity, fundus classification according to Fishman,[9] FAF group, ERG group according to Lois,[11] mfERG classification according to Kretschmann,[13] and age of patients. The results in terms of Spearman ρ and $P$ values are summarized in Table 2.

Macular thickness and age of patients did not correlate with any of the clinical parameters investigated. Of interest, no correlation was found between IS/OS abnormalities and foveal thickness (Spearman $\rho = -0.11$, $P = 0.4$; Table 2).

A significant correlation was seen between IS/OS junction preservation and better BCVA in STGD patients (Spearman $\rho = -0.43$, $P \leq 0.01$). There was also a significant direct relationship between IS/OS junction abnormalities and the degree of fundus lesions observed by fundus examination (Spearman $\rho = 0.73$, $P \leq 0.01$) and FAF imaging (Spearman $\rho = 0.76$, $P \leq 0.01$); hence, preserved IS/OS junction correlated with preserved foveal areas, as can be seen also in Figure 1.

A significant direct correlation was also observed between IS/OS preservation and better ERG and mfERG responses (Spearman $\rho = 0.49$, $P \leq 0.01$, and Spearman $\rho = 0.53$, $P \leq 0.01$; respectively).

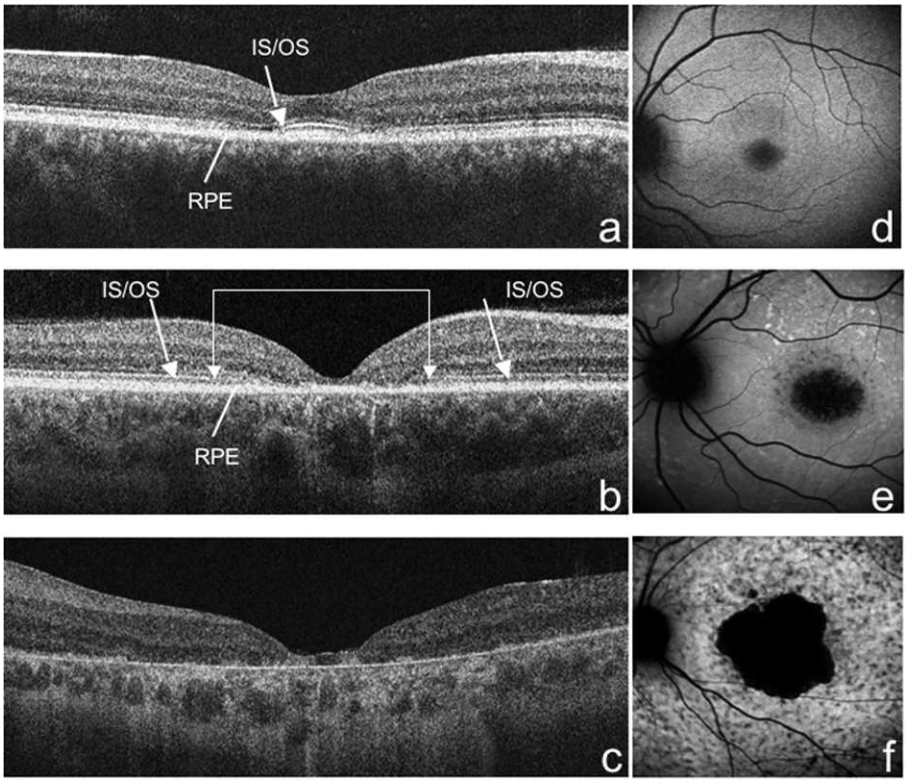


**Figure 1.** SD-OCT. (**a**) IS/OS junction disorganization in the fovea (*arrow*); (**b**) IS/OS junction loss closer to the fovea (*double arrow*) compared with the extrafoveal area (*arrows*); (**c**) extensive loss of IS/OS junction and RPE atrophy. (**d**) FAF; presence of a ring of increased autofluorescence surrounding an area of decreased autofluorescence; (**e**) absence of foveal autofluorescence (<1 disc diameter); and (**f**) absence of macular autofluorescence (≥2 disc diameter).

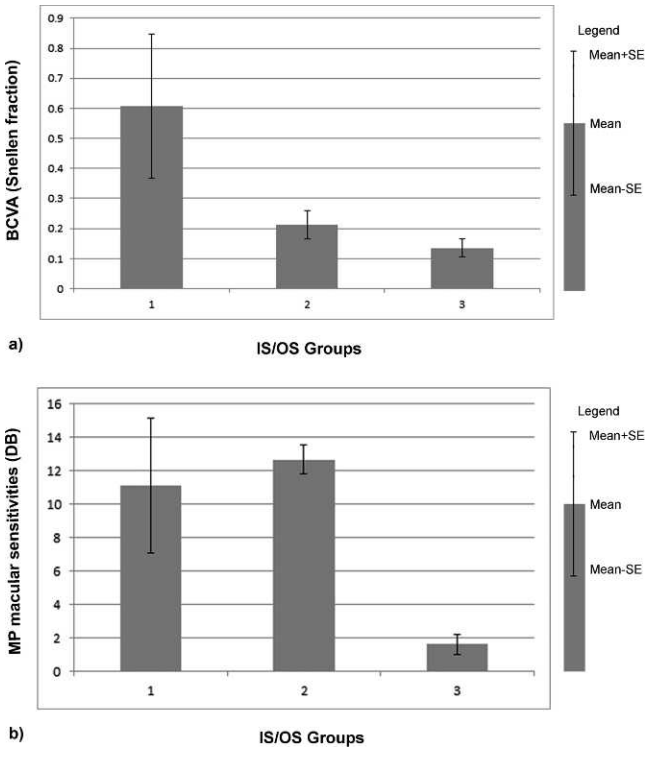


**Figure 2.** Mean ± SE data representation between IS/OS groups of photoreceptors damage and (**a**) BCVA; (**b**) MP macular sensitivities.

Finally, the degree of IS/OS preservation showed a statistically significant correlation with the amount of mean retinal sensitivity (Spearman $\rho = -0.76$, $P \leq 0.01$).

To evaluate the contribution of *ABCA4* gene mutations to the clinical manifestation of the disease, the patients previously classified into three stages by OCT were then divided into two groups to be numerically comparable: group I, with IS/OS junction disorganization in the fovea and IS/OS junction loss in the foveal area (27 patients); and group II, with extensive loss of IS/OS junction (26 patients). There was no statistically significant age difference between the two groups ($P = 0.2$; Student's *t*-test). We did not observe any significant difference in the frequency between the two groups of all missense (43 of 60 [71.7%] in group I vs. 35 of 52 [67.3%] in group II) or premature truncation mutations (17 of 60 [28.3%] in group I vs. 17 of 52 [32.7%] in group II) of the ABCA4 protein. However, we confirmed that the G1961E mutation is associated with a milder STGD phenotype, being more frequent in the stage-I group compared with the stage-II group of patients (17 of 60 [28.3%] in group I vs. 5 of 52 [9.6%] in group II; $P = 0.01$).

## Discussion

The present article reports a comprehensive clinical and genetic study of Italian Stargardt patients in addition to previously reported studies on the Italian population.[16,17]

Our study demonstrates the positive correlations between the preservation of the IS/OS junction and a better BCVA, a higher microperimetric sensitivity, a larger mfERG response, and less atrophic macular lesions, suggesting that IS/OS junction preservation can be considered a valuable marker of disease severity.

**Table 2.** Spearman Correlation between Macular Thickness and Age of Patients with the Selected Clinical Parameters

| | Age | OCT ft |
|---|---|---|
| BCVA | $P = 0.11$ ($\rho = -0.23$) | $P = 0.72$ ($\rho = -0.04$) |
| OCT ft | $P = 0.81$ ($\rho = -0.03$) | – |
| MP sensitivity | $P = 0.08$ ($\rho = -0.21$) | $P = 0.44$ ($\rho = -0.2$) |
| IS/OS category | $P = 0.42$ ($\rho = -0.11$) | $P = 0.44$ ($\rho = -0.1$) |
| Fundus classification according to Fishman et al.[9] | $P = 0.09$ ($\rho = 0.2$) | $P = 0.6$ ($\rho = -0.06$) |
| FAF group | $P = 0.18$ ($\rho = 0.2$) | $P = 0.8$ ($\rho = -0.03$) |
| ERG group according to Lois et al.[11] | $P = 0.55$ ($\rho = 0.07$) | $P = 0.9$ ($\rho = -0.01$) |
| mfERG classification according to Kretschmann et al.[13] | $P = 0.6$ ($\rho = 0.08$) | $P = 0.3$ ($\rho = -0.13$) |

BCVA, best corrected visual acuity; OCT, optical coherence tomography; MP, microperimetry; IS/OS, innerouter segment junction; FAF, fundus autofluorescence; ERG, electroretinogram; mfERG, multifocal-electroretinogram.

The clinical relevance of the IS/OS junction was actually expected since histopathologic studies in STGD patients revealed an accumulation of lipofuscin fluorophores within the RPE cells leading to loss of RPE and photoreceptors,[18] which determined visual impairment.[19,20]

OCT is a noninvasive technique based on low interferometry, which provides optical cross-sectional images of the retina and morphologic information similar to that obtained from histologic sections.[21] Changes in retinal thickness associated with IS/OS degeneration in STGD patients have been previously described using high-speed ultrahigh-resolution OCT (UHR-OCT),[22,23] and it has been demonstrated that these findings accurately correspond to those obtained using lower resolution devices such as the SD-OCT.[24]

From the comparison of structural changes assessed by SD-OCT and those observed by fundus autofluorescence,[24] it has been suggested that the structural integrity of the photoreceptors may be affected before changes occur in the RPE and that the photoreceptor function is directly affected by mutations in the *ABCA4* gene; in other words, RPE damage contributes to the degenerative process but it is not the only causative factor.

The results of the present study are in agreement with Ergun et al.[22] who analyzed the photoreceptor morphology, using UHR-OCT, in 14 patients affected by STGD and fundus flavimaculatus and demonstrated excellent visualization of intraretinal morphology, enabling the quantification of the IS/OS junction irregularities that correlate with degree of BCVA impairment. The integrity of the IS/OS junction was found to correlate also with BCVA changes in patients with a variety of other retinal diseases, including AMD, macular hole, central serous chorioretinopathy, central and branch retinal vein occlusion, diabetic macular edema, and retinitis pigmentosa.[25] Although BCVA assessment is typically used as the gold standard for assessing visual function, it is insufficient to fully characterize visual impairments because it is based on the subjective response of patients and is not a specific measure of the photoreceptor function; thus, the comprehensive clinical examination reported in the present study offers a more accurate description of the clinical features of the STGD. Based on our findings, retinal function assessed by microperimetry, ERG and mfERG, appeared to be influenced by the IS/OS junction status to a greater extent than BCVA, suggesting that IS/OS junction morphology can be considered a good indicator of photoreceptor function in STGD patients.

In the present study, it has been demonstrated that the G1961E mutation is associated with a better preserved IS/OS junction; this result also agrees with Cella et al.[26] who reported that the anatomic and functional features associated with both homozygous and heterozygous G1961E mutations are limited to changes in the parafoveal region rather than generalized retinal dysfunction.

In conclusion, SD-OCT proved to be a useful tool for the clinical assessment of STGD. Our clinical results confirm that the evaluation of the IS/OS junction in association with genotype characterization enables an accurate estimation of induced macular damage. In the present study, it has also been demonstrated that the preservation of the IS/OS junction does not correlate with retinal thickness; hence, it can be assumed that both parameters should be taken into account, particularly in the prospective of future gene therapy. A longitudinal study to better document disease progression through IS/OS junction abnormalities and its correlation with BCVA, retinal sensitivity, and macular function could validate the use of the IS/OS junction examination by OCT as a marker of disease progression and its usefulness in future clinical trials.

Restoration of vision is the ultimate goal of research on human retinal degeneration. Gene therapy for retinal pathologies is a promising field of research; in fact, animals and humans with Leber congenital amaurosis resulting from RPE65 mutation have been successfully treated with gene transfer.[27–29] However, in these cases, the rate of success depends on the amount of photoreceptors still preserved. The ability to identify and to target the retinal locations with retained photoreceptors is a prerequisite for successful gene therapy in humans. Hence, an extensive noninvasive clinical investigation performed on patients carrying *ABCA4* mutations is essential in the identification of amenable candidates for gene-based therapeutic applications.

## Acknowledgments

The authors thank Carmela Acerra for text editing. We also thank Luisa Cutillo, Annamaria Carissimo of the Telethon Institute of Genetics and Medicine (TIGEM) Bioinformatic core, and Paolo Melillo of the Department of Electronics, Computer Sciences and Systems of the University of Bologna for statistical assistance.

## References

1. Stargardt K. Über familiäre progressive degenerationen im kindesalter. *Graefes Arch Clin Exp Ophthalmol*. 1909;71:534–550.
2. Cideciyan AV, Aleman TS, Swider M, et al. Mutations in ABCA4 result in accumulation of lipofuscin before slowing of the retinoid cycle: a reappraisal of the human disease sequence. *Hum Mol Genet*. 2004;13:525–534.
3. Rotenstreich Y, Fishman GA, Anderson RJ. Visual acuity loss and clinical observations in a large series of patients with Stargardt's disease. *Ophthalmology*. 2003;110:1151–1158.
4. Armstrong JD, Meyer D, Xu S, et al. Long-term follow-up of Stargardt's disease and fundus flavimaculatus. *Ophthalmology*. 1998;105:448–458.
5. Fishman GA, Farber M, Patel BS, et al. Visual acuity loss in patients with Stargardt's macular dystrophy. *Ophthalmology*. 1987;94:809–814.
6. Allikmets R, Singh N, Sun H, et al. A photoreceptor cell-specific ATP-binding transporter gene (ABCR) is mutated in recessive Stargardt macular dystrophy. *Nat Genet*. 1997;15:236–246.
7. Sun H, Nathans J. Mechanistic studies of ABCR: the ABC transporter in photoreceptor outer segments responsible for

autosomal recessive Stargardt disease. *J Bioenerg Biomembr*. 2001;33:523–530.

8. Kiernan DF, Mieler WF, Hariprasad SM. Spectral-domain optical coherence tomography: a comparison of modern high-resolution retinal imaging systems. *Am J Ophthalmol*. 2010; 149:18–31.
9. Fishman GA, Stone EM, Grover S, Derlacki DJ, Haines HL, Hockey RR. Variation of clinical expression in patients with Stargardt dystrophy and sequence variations in the ABCR gene. *Arch Ophthalmol*. 1999;117:504–510.
10. Marmor MF, Holder GE, Seeliger MW, Yamamoto S. Standard for clinical electroretinography (2004 update). *Doc Ophthalmol*. 2004;108:107–114.
11. Lois N, Holder GE, Bunce C, Fitzke FW, Bird AC. Phenotypic subtypes of Stargardt macular dystrophy—fundus flavimaculatus. *Arch Ophthalmol*. 2001;119:359–369.
12. Hood DC, Bach M, Brigell M, et al. ISCEV guidelines for clinical multifocal electroretinography (2007 edition). *Doc Ophthalmol*. 2008;116:1–11.
13. Kretschmann U, Seeliger MW, Ruether K, Usui T, Apfelstedt-Sylla E, Zrenner E. Multifocal electroretinography in patients with Stargardt's macular dystrophy. *Br J Ophthalmol*. 1998;82: 267–275.
14. Ko TH, Fujimoto JG, Schuman JS, et al. Comparison of ultrahigh and standard-resolution optical coherence tomography for imaging macular pathology. *Ophthalmology*. 2005; 112:1922.e1–15. Available at: http://www.ophsource.org/periodicals/ophtha. Accessed June 29, 2011.
15. Midena E, Vujosevic S, Convento E, Manfre' A, Cavarzeran F, Pilotto E. Microperimetry and fundus autofluorescence in patients with early age-related macular degeneration. *Br J Ophthalmol*. 2007;91:1499–1503.
16. Simonelli F, Testa F, Zernant J, et al. Genotype-phenotype correlation in Italian families with Stargardt disease. *Ophthalmic Res*. 2005;37:159–167.
17. Sodi A, Bini A, Passerini I, Forconi S, Menchini U, Torricelli F. Different patterns of fundus autofluorescence related to ABCA4 gene mutations in Stargardt disease. *Ophthalmic Surg Lasers Imaging*. 2010;41:48–53.
18. Delori FC, Staurenghi G, Arend O, Dorey CK, Goger DG, Weiter JJ. In vivo measurement of lipofuscin in Stargardt's disease–Fundus flavimaculatus. *Invest Ophthalmol Vis Sci*. 1995;36:2327–2331.
19. Fishkin NE, Sparrow JR, Allikmets R, Nakanishi K. Isolation and characterization of a retinal pigment epithelial cell fluorophore: an all-trans-retinal dimer conjugate. *Proc Natl Acad Sci U S A*. 2005;102:7091–7096.
20. Karan G, Lillo C, Yang Z, et al. Lipofuscin accumulation, abnormal electrophysiology, and photoreceptor degeneration in mutant ELOVL4 transgenic mice: a model for macular degeneration. *Proc Natl Acad Sci U S A*. 2005;102:4164–4169.
21. Hee MR, Iyatt JA, Swanson EA, et al. Optical coherence tomography of the human retina. *Arch Ophthalmol*. 1995;113: 325–332.
22. Ergun E, Hermann B, Wirtitsch M, et al. Assessment of central visual function in Stargardt's disease/fundus flavimaculatus with ultrahigh-resolution optical coherence tomography. *Invest Ophthalmol Vis Sci*. 2005;46:310–316.
23. Srinivasan VJ, Wojtkowski M, Witkin AJ, et al. High-definition and 3-dimensional imaging of macular pathologies with high-speed ultrahigh-resolution optical coherence tomography. *Ophthalmology*. 2006;113:2054.e1–14. Available at: http://www.ophsource.org/periodicals/ophtha. Accessed June 29, 2011.
24. Gomes NL, Greenstein VC, Carlson JN, et al. A comparison of fundus autofluorescence and retinal structure in patients with Stargardt disease. *Invest Ophthalmol Vis Sci*. 2009;50:3953–3959.
25. Landa G, Su E, Garcia PM, Seiple WH, Rosen RB. Inner segment-outer segment junctional layer integrity and corresponding retinal sensitivity in dry and wet forms of age-related macular degeneration. *Retina*. 2011;31:364–370.
26. Cella W, Greenstein VC, Zernant-Rajang J, et al. G1961E mutant allele in the Stargardt disease gene ABCA4 causes bull's eye maculopathy. *Exp Eye Res*. 2009;89:16–24.
27. Maguire AM, Simonelli F, Pierce EA, et al. Safety and efficacy of gene transfer for Leber's congenital amaurosis. *N Engl J Med*. 2008;358:2240–2248.
28. Bainbridge JW, Smith AJ, Barker SS, et al. Effect of gene therapy on visual function in Leber's congenital amaurosis. *N Engl J Med*. 2008;358:2231–2239.
29. Hauswirth WW, Aleman TS, Kaushal S, et al. Treatment of Leber congenital amaurosis due to RPE65 mutations by ocular subretinal injection of adeno-associated virus gene vector: short-term results of a phase I trial. *Hum Gene Ther*. 2008;19: 979–990.